JOURNAL OF CATALYSIS 70, 123–136 (1981)

Methanol Conversion on Acidic ZSM-5, Offretite, and Mordenite Zeolites: A Comparative Study of the Formation and Stability of Coke Deposits

PIERRE DEJAIFVE, ALINE AUROUX, PIERRE C. GRAVELLE, AND JACQUES C. VÉDRINE

Institut de Recherches sur la Catalyse (CNRS), 2 Avenue Albert Einstein, 69626 Villeurbanne, France

AND

ZÉLIMIR GABELICA AND E. G. DEROUANE[1]

Laboratoire de Catalyse, Facultés Universitaires de Namur, 61 Rue de Bruxelles, 5000 Namur, Belgium

Received October 21, 1980; revised January 5, 1981

The deposition of carbonaceous residues, leading to aging and modifications in the acidic properties of three zeolite samples differing by the size and shape of their interconnecting channel networks (ZSM-5, offretite, and mordenite), has been investigated during the conversion reaction of methanol to hydrocarbons. Catalytic tests, thermogravimetry, and microcalorimetry are used as complementary techniques. For zeolite ZSM-5, it is observed that carbonaceous residues are primarily formed on the outer surface of the crystallites, resulting only in a slight modification of its molecular shape-selective properties and producing a high resistance to aging. For offretite and mordenite, by contrast, the channels are large enough to accommodate carbonaceous residues, which leads to a drastic loss of catalytic activity and a very fast aging. The intimate nature of the channel network is shown to play a determining role in the coke formation and in the ease of removal of carbonaceous deposit. The role played by the shape-selective properties of the zeolites on their behavior towards coking and aging and also the effect of coking on the availability of Brønsted acidic sites have been particularly emphasized.

INTRODUCTION

Coke formation, i.e., the deposition of carbonaceous residues, on solid acid catalysts such as silica–alumina or zeolites usually leads to their rapid deactivation (*1*). In a recent work, Rollmann and Walsh (*2*) clearly demonstrated that intracrystalline coking of zeolites is a shape-selective process which is controlled directly by the zeolite pore structure and they investigated the mechanisms which lead to coke formation (*3–5*). Clearly, a major step in the formation of carbonaceous residues is the reaction and conversion of alkylaromatics (by cyclization, dehydrogenation, further alkylation, etc.) eventually leading to polyalkylaromatics and polyaromatics which are coke precursors. The latter reactions may be prevented to a large extent by the structural constraints which are imposed in the most particular pore structure (shape and size of the channels) of ZSM-5, which explains its extremely high resistance to coking (*5*).

It is of paramount interest to relate coke formation on various catalysts to their actual rate of deactivation. Coke deposits can indeed lower the catalytic activity by site coverage (poisoning) and/or by pore blocking which prevents the access of the reactants to the active sites. Kinetics of coking were first analyzed by Voorhies (*6*), while more sophisticated models, recently developed by Beeckman and Froment (*7, 8*), consider the kinetics of catalyst aging as a function of two probabilities, namely, $P(t)$ which is the probability that an active site is

[1] To whom correspondence concerning this paper should be sent.

0021-9517/81/070123-14$02.00/0

accessible at time t and $S(t)$ which is the conditional probability that the same site is not poisoned at the same time. In the particular case of zeolites, $S(t)$ will depend on molecular shape-selective properties as they affect the coking (poisoning) rate (*2–5*), while $P(t)$ will be related to the geometry of the pore network (*9*).

The aim of the present work is to delineate the above factors in the carbon formation and in the aging of three types of zeolites which differ by the shape-selective properties and structure of their channel network. Zeolite ZSM-5 is highly shape selective (*2, 5*) and shows a three-dimensional pore structure. Mordenite has a two-dimensional channel network of which one channel however is not easily accessible; it can therefore be considered as pseudo unidimensional. Mordenite shows the same pore volume as zeolite ZSM-5. Offretite has a three-dimensional pore structure, but two of the channel systems are narrower than the third; it also possesses cages, which accounts for its larger pore volume. Due to the wider openings of their principal channel networks (see Table 1), mordenite and offretite are less molecular shape selective than zeolite ZSM-5.

Methanol conversion to hydrocarbons was used in all cases as the test reaction in view of its current interest (*10, 11*). Coking and decoking rates, i.e., the rates of deposition and removal of carbonaceous residues, were monitored by thermogravimetric analysis; ammonia adsorption and microcalorimetry were used to probe the progressive poisoning of the active sites and reaction kinetics were measured to gain insight into the relationships existing between coking and aging, with respect to activity and selectivity, for such catalysts.

EXPERIMENTAL

Materials. Three zeolites with different channel structures were used as catalysts in the present study:

(i) a synthetic small-pore mordenite, from "La Grande Paroisse" (CM-180),

(ii) a synthetic offretite (*12*) kindly supplied by Dr. C. Mirodatos and prepared by Professor R. M. Barrer,

(iii) a ZSM-5-type zeolite synthesized as previously described (*13, 14*) with particle size in the range 2–5 μm.

All catalysts were used in their protonated forms (*17*) and possessed the chemical compositions and characteristics summarized in Table 1.

Methanol was a high-purity-grade reagent (Merck >99.5% Art. 6009) used without further purification.

Catalytic studies. A fixed-bed single-flow microreactor (about 0.1 g of catalyst) was used. Following activation of the zeolites at 650 K overnight under dry nitrogen (flow rate = 1 Nl · h^{-1}), the vapor phase of thermostated liquid methanol was carried through the catalytic bed using nitrogen as vector gas (methanol : N_2 = 1 : 25). Reaction conditions were 650 K and WHSV = 10 h^{-1}.

Products were analyzed on-line by gas chromatography at various times on stream

TABLE 1

Chemical Compositions and Channel Characteristic of Zeolitic Catalysts

Zeolite	Chemical formula	Channel system[a]
H–ZSM-5	$Na_{0.03}H_{2.67}Al_{2.7}Si_{93.3}O_{192} \cdot 9\ H_2O$	(5.3 × 5.7) ↔ 5.5***
H–offretite	$Na_{0.01}K_{0.6}H_{3.0}Al_{3.6}Si_{14.4}O_{36} \cdot x\ H_2O$	6.4* ⊥ (3.6 × 5.2)**[b]
H–mordenite	$Na_{0.7}H_{4.6}Al_{5.3}Si_{42.7}O_{96} \cdot 28\ H_2O$	(6.7 × 7.0)* ⊥ (2.9 × 5.7)*

[a] Ref. (*15*). Channel dimensions in Å; (↔) interconnected channels; (⊥) perpendicular channels; number of asterisks indicates whether the channel network is one, two, or three dimensional.

[b] Offretite also has cages with dimensions 6.0–7.4 Å.

using flame-ionization detection as previously described (*10, 11*). Quantitative analyses were obtained by the determination of response factors with pure compounds used as standards. Carbon balances were calculated as percentages of total carbon in the product stream with respect to methanol as reagent in the inlet stream. Discrepancies in carbon balances, when present, indicated the occurrence of side reactions such as coke formation.

Microcalorimetry. Adsorption heats were measured using a heat-flow microcalorimeter maintained at 423 K. Calibration and ammonia adsorption procedures have been previously described (*16, 17*). Adsorption isotherms were simultaneously obtained. The amounts of adsorbed ammonia were normalized to the standard conditions of temperature and pressure. Before the calorimetric measurements, the fresh samples were evacuated overnight at 673 K down to a pressure of 10^{-4} Torr in order to desorb molecular water eventually present. Coke deposition from the methanol-to-hydrocarbons reaction was achieved by maintaining the catalytic reactor at 659 K for 20 min. The coked samples were also reactivated under vacuum at progressively increasing temperatures (423 and 673 K) before the microcalorimetric measurements.

Thermal analysis. A STA-780 Thermal Analysis System (TG,DTA,DTG) from Stanton Redcroft has been used to study the formation and removal of coke. Activation, coking, and decoking treatments were performed *in situ* in the TG system. About 0.05 g of catalyst was used in all cases. Following activation in dry N_2 (Air Liquide) at 773 K for 2 h, the furnace temperature was lowered to 650 K and a methanol–nitrogen gas mixture was passed isothermally over the sample under the same conditions as those used for the kinetic measurements.

Coke formation was directly and continuously monitored by following the gain of sample weight with time. Coke removal was achieved by increasing the sample temperature to 770 K in a dry air flow (1 $Nl \cdot h^{-1}$). This process was continuously monitored by following the weight loss vs time. Weight variations (in %) have been referred to the weight of the original (hydrated) samples at 293 K.

RESULTS

Thermogravimetric Study of Carbon Residues Formation and Removal

The deposition of carbonaceous residues and their removal have been followed by isothermal gravimetry. Figure 1 shows experimental data for all three zeolites, while Table 2 compares the coke selectivities of the various zeolites. The methanol-to-hydrocarbons reaction at 650 K was used for coking, while decoking was achieved with dry air at 770 K. The thermogravimetry data enable a quantitative comparison of the initial rates of coking and decoking of the various zeolites to be made as well as an evaluation of the maximum amounts of coke formed in each case.

Initial rates of coking, per unit mass of catalyst, are clearly increasing in the order H–ZSM-5, H–mordenite, and H–offretite. An inversion in the amounts of coke deposited occurs at about 15 min (for our experimental conditions) between H–mordenite and H–offretite. These initial rates of coking may also be expressed with respect to the actual number of Al atoms or Brønsted sites, the latter being the actual active sites, in which case it is seen that initial coking rates per acidic site are nearly identical for all three zeolites (Table 2).

Saturation by carbonaceous deposits occurs at various times on stream for the three zeolites and the maximum amounts of coke deposited are also widely different. It can be seen that the amounts of coke deposited on mordenite or offretite are almost proportional to their respective free pore volumes, while it is not so for H–ZSM-5. A simple calculation indicates that the maximum amount of coke formed on H–ZSM-5 corresponds nearly to the deposition of a polyaromatic compound (mono)layer on

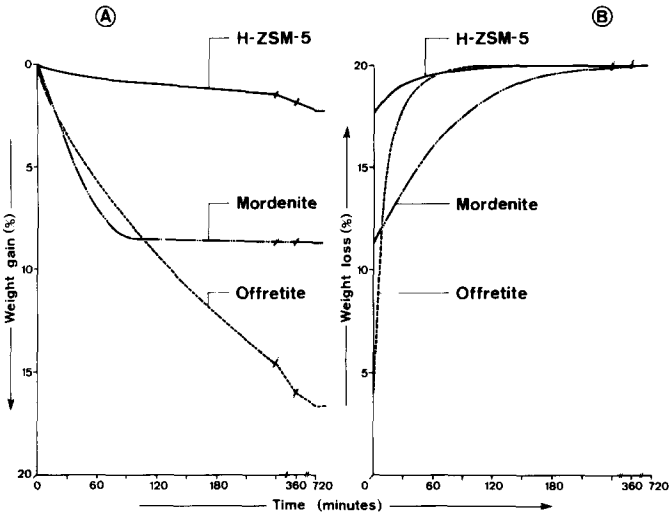

FIG. 1. (A) Formation of carbon residues from methanol conversion at 650 K on various zeolites: % weight gain vs time as followed by isothermal gravimetry. (B) Removal of carbon residues by dry air at 770 K for various zeolites: % weight loss vs time as followed by isothermal gravimetry.

the external surface of particles with diameter near 1 μm.

Carbonaceous residues were also characterized by EPR (at room temperature). For all three catalysts, linewidths are about 10 Oe although g values differ slightly. Coke on mordenite and offretite shows a g value of about 2.0026, characteristic of polyaromatic radicals, while g is about 2.0022 for H–ZSM-5, thus indicating a higher graphitic character in that case (*19*).

It is seen from Fig. 1B that apparent decoking rates (i.e., mass of coke removed per unit time) are decreasing in the order H–offretite > H–mordenite ~ H–ZSM-5. Table 3 clearly shows that there is no parallelism between these rates and the respective concentrations in framework Al atoms or Brønsted sites. As will be discussed later, the lower decoking rates of H–ZSM-5 and H–mordenite are probably due to a more hydrogen deficient nature of coke and a pseudo-unidimensional channel structure, respectively.

TABLE 2

Coke Selectivities of Various Zeolites from Isothermal Gravimetry

Catalyst	Si/Al ratio	Number of Al atoms/100 g [Number of H atoms/100 g] ($\times 10^{-23}$)	Pore volume[a] (cm^3/cm^3 cat.)	Maximum amount of coke (% wt)	Initial coking rate[b] (g/Al site · min^{-1}) [g/H site · min^{-1}] ($\times 10^{-23}$)
H–ZSM-5	34.6	0.274 [0.270]	0.29	2.2	0.164 [0.166]
H–mordenite	8.1	0.935 [0.811]	0.28	8.7	0.137 [0.154]
H–offretite	4.0	1.691 [1.409]	0.40	16.8	0.118 [0.142]

[a] Void volume in cm^3 per cm^3 of catalyst; Ref. (*18*).

[b] Rate expressed as wt coke in g per Al site per minute or, in square brackets, in g per H site per minute.

TABLE 3

Initial Rates of Removal of Carbonaceous Residues from Isothermal Gravimetry[a]

Catalyst	Rate of coke removal		
	(g/100 g) min^{-1}	(g/Al site) min^{-1}	(g/H site) min^{-1}
H–ZSM-5	0.07	0.255	0.259
H–mordenite	0.097	0.103	0.119
H–offretite	0.972	0.574	0.689

[a] P = 1 atm; dry air; T = 770 K.

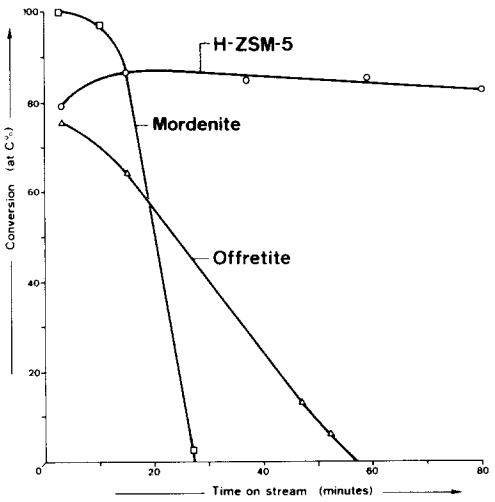

FIG. 2. Percentage of CH_3OH and DME (in equiv. CH_3OH) converted to hydrocarbon products and coke as a function of time on stream (1 atm, WHSV = 10 h^{-1}, 650 K).

Investigations of Aging during the Conversion of Methanol to Hydrocarbons

Aging of a zeolite catalyst by the formation of carbonaceous residues manifests itself in three ways:

(i) carbon balances (products vs reactants) will be deficient,

(ii) the catalytic activity (i.e., the conversion of the reactants) will progressively decrease due to the combination of site coverage and pore blocking effects (*7*),

(iii) the (shape) selectivity of the catalyst may also vary due to intimate changes in effective pore openings, cages dimensions, etc.

Figure 2 shows the methanol conversion to nonoxygenated products (hydrocarbons and possibly carbonaceous residues) as a function of time on stream. Dimethyl ether (DME) was always simultaneously present, in near equilibrium with methanol, and its concentration was converted to equivalent methanol in order to establish the overall conversion of the latter. Conversions were evaluated as the ratio (in %) of the number of C atoms in the hydrocarbon products plus discrepancies in C balances (C atoms as carbonaceous residues, see Table 4) referred to the total number of C atoms in the feed (as obtained from a bypass of methanol). Comparison of Fig. 2 and Table 4 clearly indicates that deactivation is linked to the formation of carbonaceous residues as evidenced by the deficiency in C balances. Of interest are the inversion between the conversions over mordenite and offretite (after 15–20 min, similar to that observed by TG for coke deposition) and the apparent initial increase in hydrocarbon conversion over the H–ZSM-5 catalyst. After this induction period (~15 min) during which carbonaceous residues are deposited (see Table 4), H–ZSM-5 remains remarkably stable for the methanol conversion. H–offretite shows a progressive aging, the

TABLE 4

Carbon Balances as a Function of Time on Stream

Time on stream (min)	Carbon balances[a] (%)		
	H–ZSM-5	H–mordenite	H–offretite
3	78	—	88
10	—	42	—
15	106	—	92
27	102	103	—
55	98	—	102

[a] $(C_{out}/C_{in}) \cdot 100$; WHSV = 10 h^{-1}; temperature = 650 K.

C balance being constant at about 90% until it is near totally deactivated, which corresponds to a slow and regular coking of the zeolite. For H–mordenite, the high initial activity disappears very sharply after about 10 min, and this is accompanied by a large deficiency in C balance. After 27 min of operation under our conditions, the C balance is again about 100% which is not surprising as only 2% of the methanol feed is then converted to products.

Figure 3 is a plot of the hydrocarbon yield (in %) in the outlet stream as a function of time on stream. It is rather similar to Fig. 2 thereby showing a parallelism between activity for the methanol conversion and overall selectivity to hydrocarbon products. It indicates that the coking activity of these catalysts (implicitly taken into account in the plots of Fig. 2) is directly related to their activity for converting methanol.

For all three catalysts, the product selectivity is also found to vary with aging. For example, the butanes:butenes ratio decreases progressively in all cases with time on stream, possibly reaching a stationary value (H-ZSM-5). It demonstrates that "extra" hydrogen is available in the early stages of the reaction originating from the rapid formation of aromatics (*11, 20*) or provided by methanol which can act as a hydrogen donor (*21*). While the aromatization selectivity stays nearly constant for H–ZSM-5, it decreases progressively for the other catalysts which are also observed to produce more methane as additional coke is deposited. The *para:ortho*-xylene ratio also varies greatly from catalyst to catalyst and as a function of conversion time. It is very large (>40) and slightly increases with coking time for H–ZSM-5, while it is much smaller (0.5–2) and stays nearly constant for the others. Such differences will be related to the unique shape-selective properties of zeolite ZSM-5.

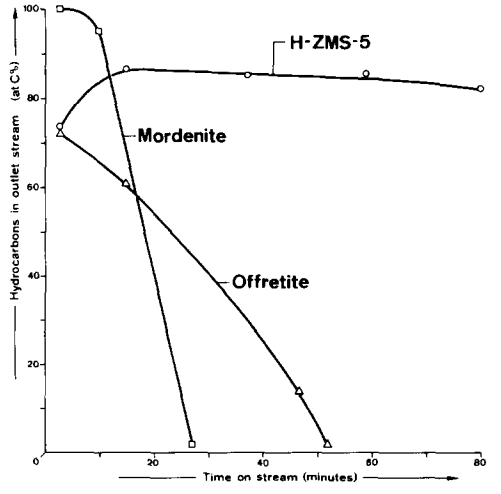

FIG. 3. Percentage of hydrocarbons in outlet stream (coke excluded) as a function of time on stream (1 atm, WHSV = 10 h^{-1}, 650 K).

Microcalorimetry

Microcalorimetry brings the following information which enables a more quantitative comparison of all three catalysts:

(i) differential heats of ammonia adsorption are measured as a function of site coverage,

(ii) adsorption isotherms are obtained simultaneously up to an equilibrium pressure of about 1 Torr,

(iii) adsorption kinetics of NH_3 are deduced from the shape of the calorimetric response curves.

The rate of ammonia adsorption (at 423 K) by H–ZSM-5 does not depend on the presence of carbonaceous deposits produced during the conversion of methanol. Coking, however, has drastic effects on both the differential heats of adsorption and the adsorption isotherms. Adsorption isotherms at 423 K, before and after coking, are shown in Fig. 4. It is clear that evacuation of the "coked" sample at 673 K before the second isotherm does not remove all the carbonaceous residues as the amount of adsorbed ammonia (at an equilibrium pressure of 0.5 Torr) is decreased by nearly 25%. It is also seen that the isotherm for the "coked" catalyst is nearly obtained by a vertical translation of the original isotherm and an ad-

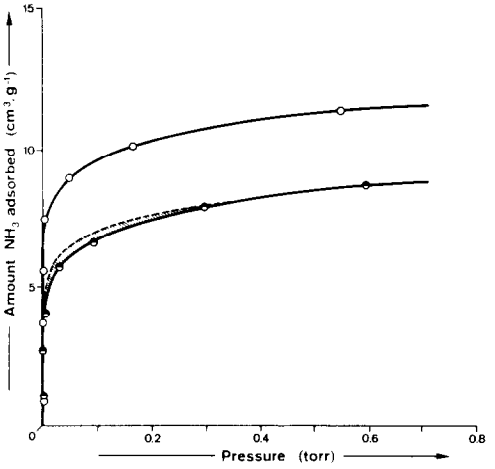

FIG. 4. Adsorption isotherms (at 423 K) of NH_3 on H–ZSM-5. ○, Fresh material activated under vacuum at 673 K; ◓, catalyst "coked" by methanol at 643 K and outgassed at 673 K. The shaded area represents the difference between the isotherm after "coking" and a vertical translation of the original isotherm.

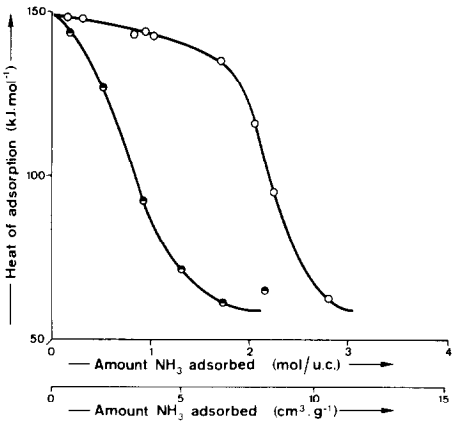

FIG. 5. Differential heats of ammonia adsorption on H–ZSM-5 (at 423 K) as a function of ammonia coverage. ○, Fresh material activated under vacuum at 673 K; ◓, catalyst "coked" by methanol at 643 K and outgassed at 673 K.

ditional decrease in ammonia adsorption in the pressure range 0.01–0.3 Torr (shaded areas in Figs. 4, 6, and 8 are used to visualize qualitatively the nature of the corresponding modifications of the isotherms). We conclude from these observations that strong and medium acidic sites are poisoned by carbonaceous residues. The latter is confirmed by considering Fig. 5 which plots the corresponding differential heats of ammonia adsorption. The ammonia adsorption capacity (by the medium and strong acidic sites, $Q_{ads} > 60$ kJ mol^{-1}) is decreased by about 40% and the strong acidic sites have been clearly poisoned to a large extent although the strongest sites ($Q_{ads} \simeq 150$ kJ mol^{-1}) are still present.

Figures 6 and 7 show the corresponding data for H–offretite. The rate of ammonia adsorption is always higher than that observed for zeolite H–ZSM-5 and it is not affected by the laydown of coke deposits. After coking and evacuation at 673 K, the adsorption isotherm of the coked zeolite appears very similar to that of the fresh material (see Fig. 6). The total adsorption capacity is only slightly decreased (8%) (note, however, that it is decreased by about 30% if the sample is reevacuated at 423 K only); some sites of medium acidity seem to have disappeared (shaded area in Fig. 6). The affinity of the coked catalyst for ammonia is however much less than the corresponding one for the fresh catalyst, as seen from Fig. 7:

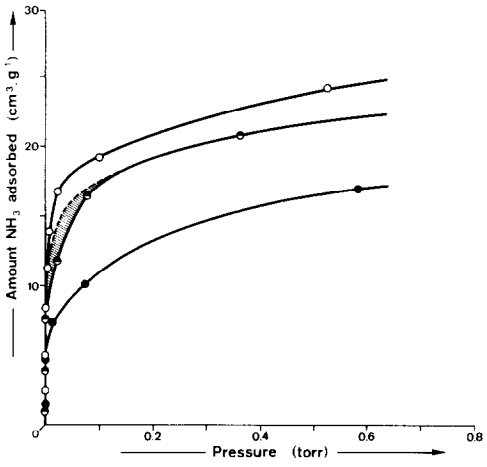

FIG. 6. Adsorption isotherms (at 423 K) of NH_3 on H–offretite. ○, Fresh material activated under vacuum at 673 K; ●, catalyst coked by methanol at 643 K and outgassed at 423 K; ◓, the same outgassed at 673 K. The shaded area represents the difference between the isotherm after coking and a vertical translation of the original isotherm.

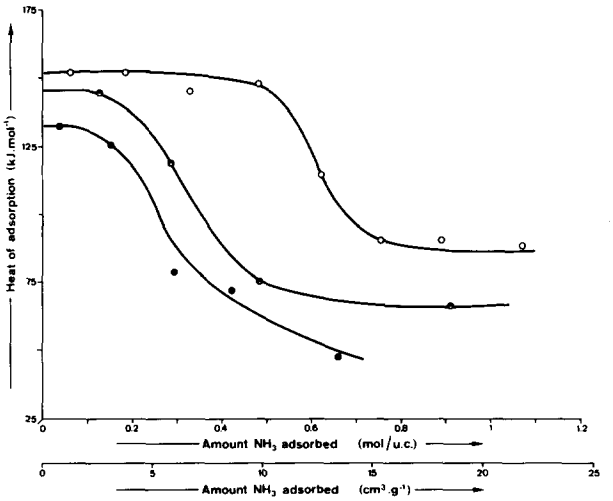

FIG. 7. Differential heats of ammonia adsorption on H–offretite as a function of ammonia coverage. ○, Fresh material activated under vacuum at 673 K; ●, catalyst coked by methanol at 643 K and outgassed at 423 K; ◓, the same outgassed at 673 K.

heats of NH_3 adsorption are smaller at all NH_3 coverages.

The situation is somewhat different in the case of H–mordenite. The fresh catalyst adsorbs ammonia (at 423 K) at a rate comparable to that of H–ZSM-5 (hence smaller than the rate observed for H–offretite). By contrast, the rate of ammonia adsorption is greatly decreased after reaction and evacuation at 673 K. In addition, production of heat has been observed after prolonged periods of apparent thermal equilibrium. This indicates that not all the acidic sites are immediately accessible to ammonia. Part of the internal surface could be available only after the disappearance of obstructions; another possible explanation could be related to a slow ordering of the adsorbed phase. The experimental observation is still not very well understood although it has been repeated several times. Figure 8 compares the adsorption isotherms (at 423 K) for the H–mordenite catalyst before and after reaction. A large decrease is observed in the ammonia adsorption capacity upon coking (40% at 0.5 Torr) and the shape of the isotherm is strongly affected, indicating

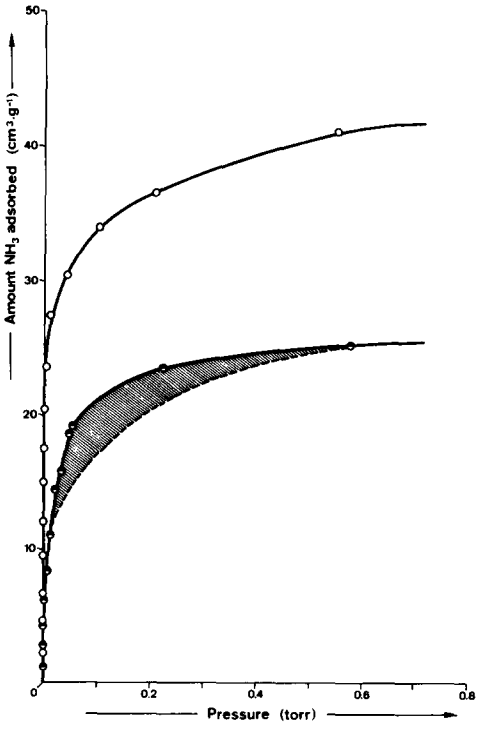

FIG. 8. Adsorption isotherms (at 423 K) of NH_3 on H–mordenite. ○, Fresh material activated under vacuum at 673 K; ◓, catalyst coked by methanol at 643 K and outgassed at 673 K. The shaded area represents the difference between the isotherm after coking and a vertical translation of the original isotherm.

that both strong and weak acidic sites have been poisoned. This is confirmed by the differential heats of adsorption plotted as a function of NH_3 coverage in Fig. 9. The adsorption is weaker in the whole range of coverage. The distribution of acidic strength also appears more heterogeneous.

DISCUSSION

The formation of carbonaceous deposits, referred to as "coke," and their consequences for catalyst acidity and activity are conveniently discussed by separating local (active site poisoning) and structural (molecular shape-selectivity) factors.

Shape-Selectivity Dependence of Intracrystalline Coking

Variations in the (Si : Al) ratio, i.e., the concentration of acidic sites, cannot explain differences in aging behavior. Indeed, *initial coking rates per acidic site* (see Table 2) *are constant* for all three catalysts within about 10%. Although this could seem surprising in view of the complexity of the methanol-to-hydrocarbons conversion reaction (*11, 20, 21*), such an agreement supports the proposal that coking behavior is essentially determined by some factor other than the Al content (*3*) and that the methanol conversion must occur on all three catalysts along closely similar reaction pathways.

By contrast, shape-selective effects are directly related to the maximum amounts of coke which are deposited. Although H-mordenite and H-ZSM-5 have identical pore volumes, the latter obviously accommodates much less coke. Recalling that bulky polyalkylaromatics which act as coke precursors are not easily formed inside H-ZSM-5 because of restricted transition-state molecular shape selectivity (*5, 22*) and our observation that the amount of coke deposited corresponds nearly to a polyaromatic hydrocarbon monolayer on the external surface of the crystallites, we must conclude that the deposition of carbonaceous residues on ZSM-5 occurs essentially on its external surface. This explains the rapid initial external coking of H-ZSM-5 followed by a very slow deactivation, its rather easy regeneration (*23*), and the fact

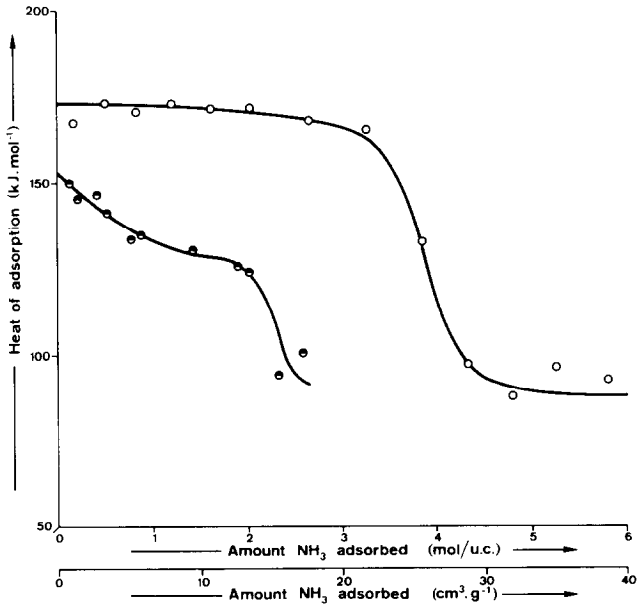

FIG. 9. Differential heats of ammonia adsorption on H-mordenite as a function of ammonia coverage. ○, Fresh material activated under vacuum at 673 K; ◓, catalyst coked by methanol at 643 K and outgassed at 673 K.

that the rate of ammonia adsorption by the internal acidic sites is barely affected by its partial coking. By contrast, a comparison of the amounts of coke deposited on H–offretite and H–mordenite shows that these vary in the same way as the corresponding void pore volumes. Intracrystalline coking obviously takes place for these two catalysts, although probably to a smaller extent in their secondary smaller channels which do not allow the formation of cycloparaffinic coke precursors (*3*). Intracrystalline coking will of course deeply affect the catalytic properties of these materials. As initial coking rates per acidic sites are identical for all catalysts, it must also be concluded that coke precursor molecules are generated everywhere in the intracrystalline void volume for all three zeolites. These have to migrate to the outer surface of the crystallites before being deposited as coke in the case of H–ZSM-5. The rate-determining process for the deposition of carbonaceous residues from methanol in zeolites then appears to be one or more of the steps leading to the formation of coke precursors such as alkylmonoaromatics, although the dehydrocyclization of the latter to polyaromatics may also be sterically impeded inside the zeolite (such as for ZSM-5) due to molecular shape selectivity.

Shape-Selective Effects in the Removal of Coke

Here also, *structural effects* need to be invoked to account for the observed variations in *decoking rates* as no direct relationship exists (as expected) with the density of acidic sites (see Table 3). Initial rates increase in the order H–mordenite < H–ZSM-5 < H–offretite. "External" coke on H–ZSM-5 was found (by EPR) to be more graphitic in nature than "internal" coke on H–offretite and H–mordenite. This observation by itself can account for the lower specific initial "decoking" rate of zeolite ZSM-5 compared to H–offretite as it is expected that the ease of removal of hydrocarbon carbonaceous deposits decreases with their hydrogen content (or H/C ratio). The difference between H–offretite and H–mordenite is however related more intimately to their structures. Mordenite must be considered as a pseudo-unidimensional channel structure while offretite has a two-dimensional secondary channel network. Removal of carbonaceous residues is intimately linked with the availability of oxygen (as decoking agent) as evacuation at 673 K barely removes coke deposits. Hence, a possible explanation (which is in agreement with the NH_3 adsorption data) is that the secondary channels of offretite stay rather free from coke and allow a better access to coke deposits (or acidic sites) by oxygen (or ammonia).

"External" coke on H–ZSM-5 will be deposited under hydrogen-deficient conditions compared to intracrystalline coke as observed for H–offretite and H–mordenite. Indeed, in the latter case coke is deposited in the presence of hydrogen released in the course of aromatization reactions (*10, 11*). This could explain the higher graphitic character of the coke deposited on zeolite H–ZSM-5 (*19*) which is however most readily regenerated without irreversible modification of the active (acidic) sites (*23*).

Poisoning and Blockage of the Active Sites

For H–ZSM-5, coking does not impose restriction to the access (by ammonia) of the active sites inside the framework as evidenced by microcalorimetry. The anomalous behavior of the ammonia adsorption heats for the fresh catalyst was previously attributed (*16*) to a heterogeneous distribution of the acidic sites combined with an immobile adsorption of ammonia, the most "energetic" sites being located at internal areas not readily accessible during adsorption. These anomalies disappear for the aged catalyst and the remaining strong acid sites (although reduced in number) have a comparable strength to that before reaction. Hence, poisoning of acid sites during the methanol conversion must mainly affect

sites of medium acidity, possibly comparable to those leading to an NH_3 temperature-programmed desorption peak at $T_{max} \sim 473$ K (β state) (*24*). As "internal" coking cannot take place in ZSM-5, the observed decrease in the number of available medium acidic sites should then be attributed to blockage of the latter by hydrocarbon residues which were not converted to aromatics (easily desorbed (*20*)), due to their lower acidity. For *offretite*, microcalorimetry data as well as adsorption isotherms clearly indicate a moderate inhibition towards the adsorption of ammonia which can be explained if carbonaceous residues are *mainly deposited in the cages and larger channels*, while the secondary channel system still provides access to the acidic sites which are partially neutralized by the carbonaceous deposits. In the particular case of *mordenite*, the ammonia adsorption is strongly inhibited by coking, *obstructions* to the access of strong acid sites seem to occur (or possible phase rearrangement), and an overall decrease in the ammonia adsorption affinity and capacity is observed. The pseudo-unidimensional channel structure of mordenite can partly explain these observations. Indeed, molecular diffusion in a pore (or channel) will be strongly inhibited when restricted (by carbonaceous deposits) at any location in the pore if the channel system is unidimensional and does not provide facilities for other access pathways.

It is obvious from Fig. 2 that absolute aging rates increase in the order H–ZSM-5 < H–offretite < H–mordenite. This can follow if it is assumed that the active-site deactivation functions, $S(t)$, are nearly the same in all cases (as evidenced by the closely identical initial coking rates), while the accessibility function, $P(t)$, to the active site will of course decrease in the order H–ZSM-5, H–offretite, H–mordenite as discussed earlier and as evidenced from the coke formation, ammonia adsorption, and microcalorimetry data. Such data are best compared by plotting the normalized hydrocarbon yields (with respect to the extrapolated yield at time $t = 0$) as functions of the relative amount of coke formed, and this is shown in Fig. 10. The normalized deactivation sequence hence appears as H–ZSM-5 < H–mordenite < H–offretite. The initial hydrocarbon yield deficiency (for H–ZSM-5) and the lower apparent hydrocarbon yield (i.e., faster aging) for offretite must be attributed to an extremely rapid coking of the external surface in the case of ZSM-5 and a high carbonaceous residue (production) capacity for offretite, the latter being able to accommodate a larger amount of coke due to its larger void pore volume.

Effect of Coking on Reaction Selectivity

Changes in catalyst selectivities may be interpreted along the same lines. High olefinic-to-paraffinic ratios correspond to hydrogen-deficient conditions in the methanol conversion and are observed when little aromatization takes place, even more as olefins through conjunct polymerization lead ultimately to aromatic hydrocarbons (*10, 11*). High yields in saturated compounds are observed when methanol acts

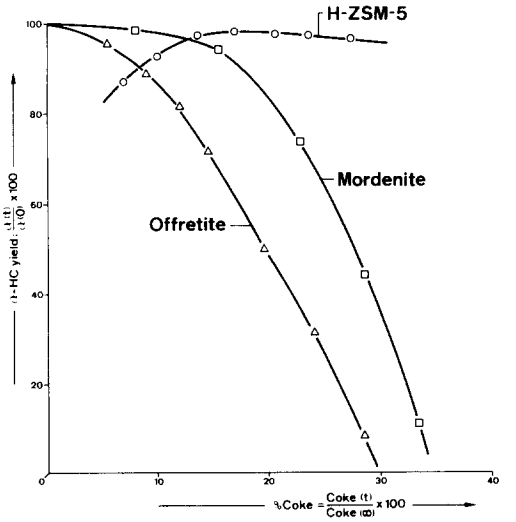

FIG. 10. Methanol conversion to hydrocarbons as a function of the relative amount of coke deposited on the three types of zeolite samples. α: ratio of hydrocarbon yield at time "t" to that extrapolated to $t = 0$.

as hydrogen donor (*21*) or when extra hydrogen is available due to the extensive occurrence of carbon deposition reactions (*11*). Aromatic yields vary with aging. Lower aromatic yield may eventually be observed if extensive coking occurs as aromatic molecules act as coke precursors but their yield also decreases progressively with coking (for H-mordenite and H–offretite). It may be explained by the progressive poisoning of the strongest acid sites as evidenced from the microcalorimetry data, which were postulated to be responsible for the aromatization of lower aliphatics (*11*), or by a relative increase in space velocity as the number of available sites decreases due to poisoning. This is less striking for H–ZSM-5 for which coking essentially occurs on the external surface. The higher selectivity of H–ZSM-5 for the formation of *p*-xylene (at least when large crystallites are used) when compared to mordenite or offretite is expected from its shape-selective properties (*25*). As coke is progressively deposited on its external surface, pore-mouth restrictions will partially occur and slightly enhance its apparent molecular shape selectivity as experimentally observed by the increasing yield in *p*-xylene.

Finally, it is interesting to note that larger amounts of methane are produced on the coked catalysts. Methane could be formed through radical reactions as proposed by Zatorski and Krzyzanowski for H–mordenite (*26*). Another possibility, however, is that methanol or dimethyl ether can act as a hydrogen transfer agent in reactions such as

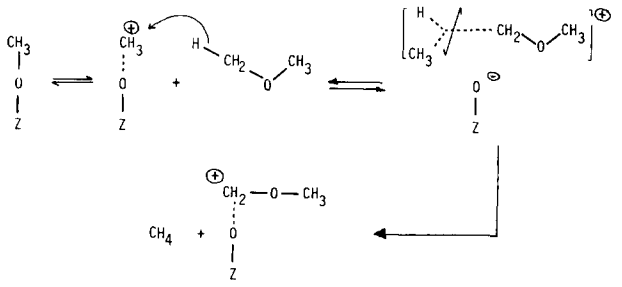

(1)

The $^{+}CH_2-O-CH_3$ species formed in this way react further, isomerize, or eventually lead to lighter products (H_2, CO, CO_2). The hydrogen (hydride) donor properties of methanol or dimethyl ether were clearly demonstrated previously (*21*). On coked catalyst, the only reaction that is observed is the methanol–dimethyl ether equilibration; it may be that, at the temperature (650 K) at which it can then be performed rather selectively, reaction (1) now becomes more important. This contrasts with what is observed on H–ZSM-5 catalyst where due to the low coke yield the activity to the formation of hydrocarbon is maintained and species like CH_3^{+} (or Z–O–CH_3) or $^{+}CH_2-O-CH_3$ will readily react further.

CONCLUSIONS

The present investigation has shown that the coking and aging behavior of zeolites is essentially determined by their structural (molecular shape-selective) properties. The initial coking activities are directly related to the availability of acidic sites, while the consequent coking and aging rates depend on the pore size and the nature of the channel network.

Intracrystalline coking takes place for both H–mordenite and H–offretite; the latter can accommodate more carbonaceous

residues due to its larger void pore volume. As a consequence, aging takes place, faster in the case of mordenite where obstructions seem to be created following coke deposition. In the particular case of offretite, the secondary channel network does not seem to have been affected to a large extent by coke deposits (no effect on ammonia adsorption rate) which can explain the rapid regeneration of the latter if oxygen still has a free access to the coke deposits in the cages and main channels. For H–ZSM-5, carbonaceous residues are deposited on the outer surface of the crystallites eventually leading to slight modifications in its (shape) selectivity towards para-aromatic compounds. Coke is however more graphitic in nature in this case, possibly as it is deposited under greater hydrogen deficient conditions. This probably explains why although it can be completely removed, coke on ZSM-5 shows a smaller initial removal rate than coke on offretite.

As to the location of the coke deposits in the various catalysts, as well as to their structural features, it is seen that the apparent acidity of the catalysts (strength and number of acidic sites, affinity for bases) is modified in different ways. No restriction of access to the acid sites (by ammonia) is observed for H–ZSM-5 and H–offretite but obstructions appear for H–mordenite. Acid strength distributions are altered in all cases. However, in the particular case of H–ZSM-5, the strongest acidic sites are still present which indicates that they are located in the intracrystalline volume of the crystallites where little coke is formed due to shape-selective restrictions. It was proposed earlier that they were located at channel intersections (*14, 20*). Coking for H–ZSM-5 zeolite could therefore be limited by increasing particle size, which decreases external surface, or by decreasing external surface acidity, for instance, by decreasing drastically the aluminum content in the last stage of crystallization. The latter process was shown (*27*) to increase the shape selectivity of ZSM-5 by inactivating its external surface with an isocrystalline layer of aluminum-free zeolite.

ACKNOWLEDGMENTS

The authors thank Dr. C. Mirodatos and Professor R. M. Barrer for the sample of synthetic offretite. P.D. acknowledges support from CNRS (France) and the Ministry of Cultural Affairs (Belgium).

REFERENCES

1. Butt, J. B., *Advan. Chem. Ser.* **109,** 259 (1972).
2. Rollmann, L. D., and Walsh, D. E., *J. Catal.* **56,** 139 (1979).
3. Rollmann, L. D., *J. Catal.* **47,** 113 (1977).
4. Walsh, D. E., and Rollmann, L. D., *J. Catal.* **49,** 369 (1977).
5. Walsh, D. E., and Rollmann, L. D., *J. Catal.* **56,** 195 (1979).
6. Voorhies, A., Jr., *Ind. Eng. Chem.* **37,** 318 (1945).
7. Beeckman, J. W., and Froment, G. F., *Ind. Eng. Chem. Fundam.* **18,** 245 (1979).
8. Beeckman, J. W., and Froment, G. F., *Chem. Eng. Sci.* **35,** 805 (1980).
9. Derouane, E. G., *in* "Intercalation Chemistry" (M. S. Whittingham and A. J. Jacobson, Eds.), Academic Press, New York, in press, 1981.
10. Dejaifve, P., Védrine, J. C., Bolis, V., Van Hooff, J. H. C., and Derouane, E. G., *Amer. Chem. Soc. Div. Petrol. Chem. Prepr.* **24,** 286 (1979).
11. Dejaifve, P., Védrine, J. C., Bolis, V., and Derouane, E. G., *J. Catal.* **63,** 331 (1980).
12. Mirodatos, C., Ph.D. thesis, Lyon, 1977, No. 77-34.
13. Argauer, R. J., and Landolt, G. R., U.S. Patent 3,702,886 (1972).
14. Derouane, E. G., B. Nagy, J., Dejaifve, P., Van Hooff, J. H. C., Spekman, B. P., Naccache, C., and Védrine, J. C., *C.R. Acad. Sci. Paris Ser. C* **284,** 945 (1977), and *J. Catal.* **53,** 40 (1978).
15. Meier, W. M., and Olson, D. H., Atlas of Zeolite Structure Types." International Zeolite Association, 1978.
16. Auroux, A., Wierzchowski, P., and Gravelle, P. C., *Thermochim. Acta* **32,** 165 (1979).
17. Auroux, A., Bolis, V., Wierzchowski, P., Gravelle, P. C., and Védrine, J. C., *J. Chem. Soc Faraday Trans II* **75,** 2544 (1979).
18. Garwood, W. E., Caesar, P. D., and Brennan, J. A., U.S. Patent 4,150,062 (1979).
19. Derouane, E. G., and Gabelica Z., unpublished results.
20. Derouane, E. G., and Védrine, J. C., *J. Mol. Catal.* **8,** 479 (1980).
21 Dejaifve, P., Ducarme, V., Védrine, J. C., and Derouane, E. G., submitted for publication.

22. Wierzchowski, P., Garbowski, E. D., and Védrine, J. C., *J. Chim. Phys.*, in press.
23. Voltz, S. E., and Wise, J. J., ERDA Report FE-1773-25, November 1976.
24. Topsøe, N. Y., Pedersen, K., and Derouane, E. G., *J. Catal.* **70**, 41 (1981).
25. Chen, N. Y., Kaeding, W. W., and Dwyer, F. G., *J. Amer. Chem. Soc.* **101**, 6783 (1979).
26. Zatorski, W., and Krzyzanowski, S., *Acta Phys. Chem.* **24**, 347 (1978).
27. Rollmann, L. D., U.S. Patent 4,148,713 (1979).